International Core Journal of Engineering Volume 11 Issue 5, 2025
ISSN: 2414-1895 DOI: 10.6919/ICJE.202505_11(5).0031

Hard Carbon Composite Material Prepared by Mixing Corn Starch with Citric Acid as Negative Electrode for Sodium Ion Batteries

Jiaqian Liu[1,2,*]

[1] School of Physics and Optoelectronic Engineering, Guangdong University of Technology, Guangzhou 510006, China

[2] The State Key Laboratory of Precision Electronic Manufacturing Technology and Equipment, School of Electromechanical Engineering, Guangdong University of Technology, Guangzhou 510006, China

Abstract

Corn starch is regarded as one of the most promising negative electrode materials for sodium-ion batteries, given its abundance, low cost and environmentally friendly composition. Nevertheless, the utilization of hard carbon anodes derived from biomass materials is constrained by the restricted capacity and low initial coulombic efficiency. In this study, corn starch was combined with varying quantities of citric acid and subjected to a series of pre-oxidation and calcination treatments with the objective of enhancing the agglomeration and foaming properties of the corn starch. The resulting batteries exhibit a high capacity and a markedly high first coulombic efficiency. The findings of this study may provide new ideas and methods for the design of sodium-ion batteries using corn starch as a precursor.

Keywords

Hard Carbons; Sodium-Ion Batteries; Anode; Biomass.

1. Introduction

Compared to the past, battery resources have changed significantly. Due to the depletion of resources, limited material development, coupled with the deterioration of the global environment and other reasons, people's expectations of the technology level and quality of batteries have increased significantly (Dong et al., 2022). With the gradual deepening of battery research, lithium-ion batteries have gradually lost their bright halo (Tan et al., 2023) and been replaced by many other battery materials (Chen et al., 2023). On the one hand, there are abundant natural energy sources such as solar energy, wind energy, tidal energy, etc., and on the other hand, there are abundant and easy-to-use materials such as Sulphur compound batteries (Yan et al., 2020; Yu et al., 2013), iron compound batteries (Wang et al., 2017), etc. Among these batteries, however, sodium-ion batteries are the most popular. as the reason of the material used in sodium-ion batteries: sodium batteries, sodium not only has the advantages of abundant reserves, low cost and easy access to materials, but also sodium and lithium belong to the same main group in the periodic table (Fan et al., 2024), so they have similar chemical properties and working principles (Nayak et al., 2018). This provides many similar research methods and ideas for using sodium as the anode of the battery, making sodium-ion batteries generally regarded as one of the most promising replacements for lithium-ion batteries in the industry.

Sodium-ion batteries generally use graphite as an anode material. Biomass carbon material is a kind of anode material that can enhance the performance of sodium-ion batteries and reduce the cost of sodium-ion batteries. It is an environmentally friendly and inexpensive carbon material (Moctar et al., 2018). The corn starch used in this paper is a typical biomass carbon material. In comparison with

ISSN: 2414-1895 DOI: 10.6919/ICJE.202505_11(5).0031

other biomass precursors, such as cellulose, lignin, sucrose, etc. (Cao et al., 2017; Wang et al., 2021; Wang et al., 2023), starch exhibits a natural spherical morphology (Li et al., 2011).

It is a typical polysaccharide with not only a simple composition (Chen et al., 2022), but also a very high carbon content, which renders it an ideal carbon precursor for the study of the chemical transformation mechanism of the material. In this paper, novel corn starch-based composites were prepared by high-temperature calcination pre-oxidation, combining the advantages of corn starch biomass carbon and citric acid. These composites were then applied to the anode of sodium-ion batteries, after which a set of discussions of the relevant battery properties was conducted.

2. Experimental

2.1 Material Synthesis

As illustrated in Fig. 1, a precise quantity of corn starch was selected and subjected to a drying process in a 55°C oven for a duration of one week, with the objective of achieving complete desiccation. In a mortar, 2 g of citric acid was manually ground and crushed into a powder, then 10 g of dried corn starch powder was added and thoroughly mixed with the citric acid powder. The mixture was subsequently placed in a corundum crucible and transferred to a tub furnace for air pre-stabilization, producing a black bulk solid pre-stabilized corn starch hard carbon composite (CAHC-0.1). The black bulk solid was transferred to a mortar and manually ground for 10 minutes to a black powder state; the black powder in the above mortar was placed in an ark for reaction; after the reaction was completed and cooled down to air temperature, the ark was removed and the black bulk product was manually ground finely to a powder state in a mortar; after grinding sufficiently, the black powder was again placed in an ark and reacted under an N2 circumstance. Following the completion of the reaction and subsequent cooling to room temperature, the black lumpy product was transferred to the mortar and manually ground to a black powder to yield the porous corn-hard carbon composite CAHC-0.1.

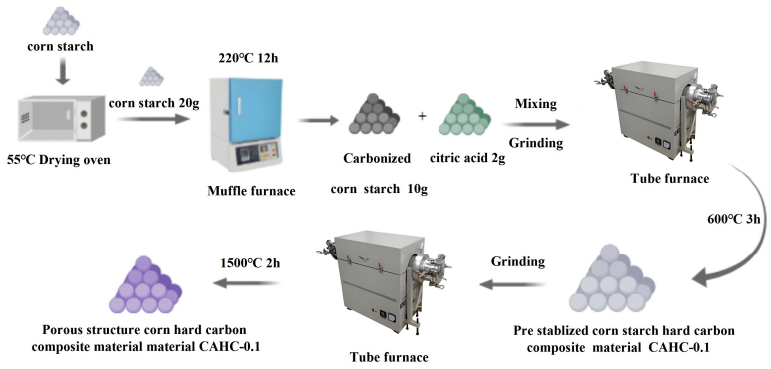

Fig. 1. Fabrication process of corn starch hard carbon composites

2.2 Battery Assembly Process

The investigation involved the utilization of a CR2032-type button sodium battery to assess the electrochemical properties of the subject. The assembly process was meticulously executed within an argon-filled glove box to ensure the integrity of the experimental environment. The diaphragm

ISSN: 2414-1895 DOI: 10.6919/ICJE.202505_11(5).0031

comprised a Celgard 2400 microporous polyethylene membrane, while the electrolyte consisted of 1.0 M LiPF6, dissolved in a 1:1 volume ratio of EC to DEC. For the sodium cell, the electrolyte was 1.0 M NaPF6 dissolved in an organic solvent, DIGLYME (diethylene glycol-dimethyl ether), and the diaphragm was a Whatman glass fibre filter paper.

The experiment was assembled by means of reverse mounting. Following the preparation of the experimental drugs, the glove box was accessed. Initially, the negative shells were arranged in a flat configuration according to the specified quantity. Subsequently, the sodium tablets were positioned face up within the negative shells following the removal of the sodium tablets' packing septum using pointed tweezers. The cut septum was then covered with the sodium tablets. The next stage of the procedure involved the use of a disposable rubber-tipped dropper to apply 4-5 drops of electrolyte to the diaphragm, ensuring its adequate moistening. The vacuum-dried pole piece, with the carbon side facing downwards, is then placed on the diaphragm, with the objective of positioning it centrally within the battery. Subsequent to this, the spacer and shrapnel should be placed in turn, and finally, the positive shell should be covered and the battery firmly pressed in the pressing machine. The completed assembly should then be placed in the constant temperature drying box for the drying process.

2.3 Electrochemical Testing

The scanning electron microscope (SEM) model Sigma300 (Carl Zeiss, Germany) was utilised for the observation and detection of the pore shape of the material. The XRD model XRD-6100 (SHIMADZU, Japan) was employed for the analysis. The Raman model DRX 2xi, manufactured by Thermo Fisher, U.S.A., was utilised to detect the material by microporous conditions. The BET model Autosorb-IQ2, manufactured by Quantachrom, U.S.A., was employed to detect the material. Quantachrom, USA, the materials were examined under microporous conditions.

3. Results and Discussion

As illustrated in Figs 2(a) through 2(c), the electron micrographs depict the sintering process of pure cornstarch hard carbon material. Figs 2(d)-(f) illustrate the scanning electron micrographs of the composite CAHC-0.1, and Figs 2(h)-(j) depict the scanning electron micrographs of the composite CAHC-0.5. An analysis of Fig. 2(a)-(c) reveals that the pure corn starch itself, after being subjected to firing without the addition of any organic components, exhibits a relatively flat surface with a paucity of pore structures. As illustrated in Fig.2(b), the sintering of pure corn starch at elevated temperatures does not result in significant agglomeration, predominantly manifesting as a laminar structure with a dispersed distribution. The images of the composite material CAHC-0. It is evident that the number of pore structures on the surface of material CAHC-0.1 is significantly enhanced, exhibiting a wide range of sizes and a high degree of density. This outcome demonstrates that the addition of citric acid has effectively facilitated the creation of pores in the original pure corn starch material. This finding suggests that the abundant microporous structure (Kumaresan et al., 2021). (especially the pore structure formed by the curved stacked carbon layers surrounded by the pore structure) could accommodate more Na+ (Wang et al., 2024) stored in the hard carbon (Shen et al., 2024), which was more favourable to the transfer and diffusion of Na+ and thus led to the improvement.

The morphology and structure of the electrode materials were characterized by TEM. Fig. 3(a) shows that the carbon crystal plane spacing of CAHC-0.1 is as high as 0.363 nm, which is much larger than that of graphite, suggesting that the firing of corn starch and citric acid together contributes to the increase of the carbon crystal plane spacing (Gao et al., 2018), which is more suitable for the storage and migration of sodium ions. The elemental mapping photographs of CAHC-0.1 (Fig. 3, c-f) demonstrate the uniform distribution of elements C, N and O within the material, indicating a uniform distribution of citric acid within the corn starch matrix. This uniform distribution is crucial for ensuring the stability of the composite (Kumar et al., 2021), which is beneficial for enhancing battery performance and stability (Zhu et al, 2019).

ISSN: 2414-1895 DOI: 10.6919/ICJE.202505_11(5).0031

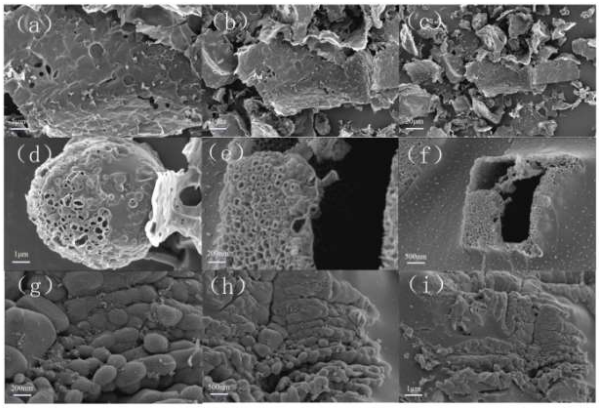

Fig. 2. (a)-(c) SEM electron micrograph of the composite HC; (d)-(f) electron micrograph of the composite CAHC-0.1; (g)-(j) SEM electron micrograph of the composite CAHC-0.5

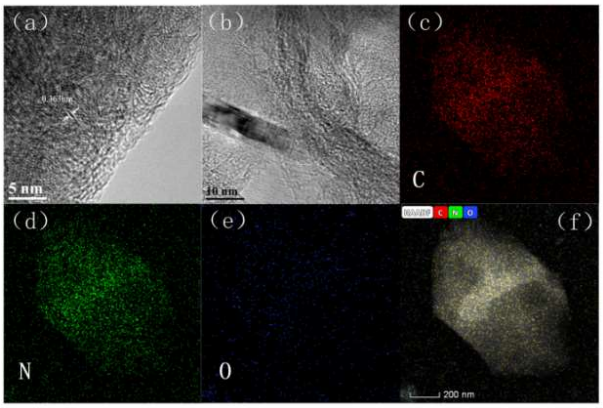

Fig. 3. TEM electron micrograph of the composite CAHC-0.1

As illustrated in Fig. 4, the XRD patterns of the composite CAHC-0.1 and pure corn starch HC exhibit two distinct diffraction peaks, located at approximately 23° and 43°, respectively. These two peaks correspond to the (002) and (100) crystal planes of graphite (Yin et al, 2024). The broadness of the diffraction peaks indicates that CAHC-0.1 is highly disordered (Pang et al., 2024).This is This is in accordance with the typical structural feature that hard carbon is mainly disordered. The layer spacing (d002) of CAHC-0.1 was found to be 0.381 nm (Kim et al., 2017) by Bragg calculations. The layer spacing of the composites was gradually reduced with the increase of the refining temperature, but all of them were larger than that of the standard layer spacing of graphite, which is 0.335 nm. The larger layer spacing is conducive to the storage and diffusion of sodium ions in the micro-crystalline structure of hard carbon (Zhang et al., 2017). Consequently, the composite CAHC-0.1 exhibits superior performance in comparison with pure corn starch (see Fig. 5, which illustrates the Raman spectra of the composite CAHC-0.1 and pure corn starch HC). Two characteristic wave peaks, the D peak and the G peak, can be observed at 1350° and 1590°, respectively. The D peak corresponds to the structural defects in the carbon lattice, while the D peak represents the expansion and contraction vibration within the sp2 hybridized carbon atomic plane in the ordered carbon structure (Arie et al., 2019). The intensity ratio of the D and G peaks (ID/IG) is a commonly used metric to assess the degree of disorder or graphitization (Li et al., 2021) of carbon materials. A larger intensity ratio (ID/IG) indicates a greater degree of structural disorder in the material, and a high degree of graphitization can enhance the multiplicative properties of hard carbon (Wang et al., 2020). The calculated ratios for CAHC-0.1, CAHC-0.5, and HC are 1.10, 0.725, and 1.065, respectively. This indicates that the degree of disorder and the degree of graphitization of the carbon material within CAHC-0.1 is relatively large (Li et al., 2018). Therefore, it can be concluded that doping 2g HC is a more appropriate choice.

ISSN: 2414-1895 DOI: 10.6919/ICJE.202505_11(5).0031

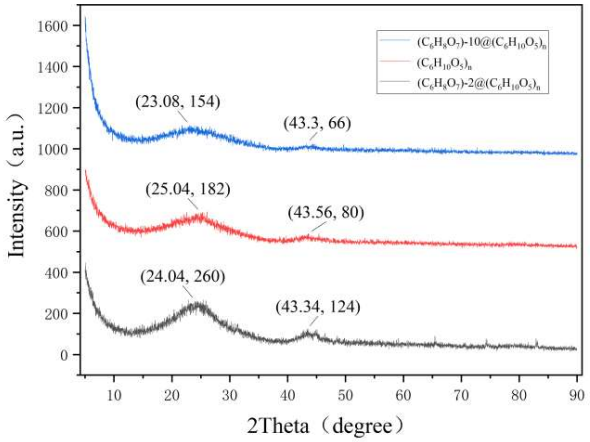

Fig. 4. Comparison diagram of XRD between CAHC-0.1and HC of the multiplicity performance of sodium-ion batteries

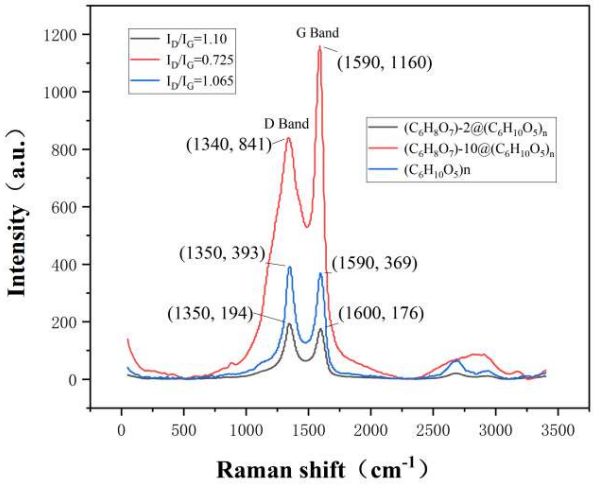

Fig. 5. Raman spectra of HC, CAHC-0.1 and CAHC-0.5

The isothermal curves of N2 desorption and pore size distributions of pure corn starch and materials CAHC-0.1 and materials CAHC-0.5 are shown in Fig. 6. From Fig. 6(a), it can be seen that the isothermal desorption curves of pure corn starch have a larger rise, while the curves of CAHC-0.1 have a steady rise relatively, all samples have a small specific surface area. This is a very good phenomenon because a low specific surface area is favorable for improving the first round Coulomb efficiency of corn starch hard carbon composites (Guo et al., 2022).

Table 1. BET results of HC, CAHC-0.1 and CAHC-0.5

Samples	BET surface area ($m^2 g^{-1}$)	Total pore volume ($cm^3 g^{-1}$)
HC	98.038	3.409
CAHC-0.1	6.598	0.002
CAHC-0.5	0.397	0.005

As illustrated in Fig. 6(b), the adsorption isotherms of CAHC-0.1 and CAHC-0.5 exhibit a type III behaviour, as reported in (Lakienko et al., 2022). Specifically, CAHC-0.1 achieves an adsorption capacity of 11.2 m3g-1 at a P/P0 ratio of 1.0, while CAHC-0.5 attains a significantly lower adsorption amount of 0.4 m3g-1 under the same conditions. The adsorption amount is comparatively negligible

ISSN: 2414-1895 DOI: 10.6919/ICJE.202505_11(5).0031

in relation to that of pure corn starch, with the adsorption amount of the pure corn starch HC at P/P0=1.0 reaching 72.6 m3g-1. However, its image does not exhibit a closed image at P/P0=0.6. One hypothesis for this phenomenon is that the functional group of pure phase corn starch is more special, which will lead to the adsorbed gas molecules can not be completely detached (Zhang et al., 2021), i.e., which is conducive to the adsorption of sodium ions but not conducive to the desorption of sodium ions, and in general is unfavorable for the transport of sodium ions. This suggests that it is most important to find the right amount of doping to enhance the performance of the Talent material first, and for this experiment (Lin et al., 2019), doping citric acid with 2g is the most preferred. As illustrated in Fig. 6, the majority of pure corn starch (HC) is concentrated between 0 and 25 nm, while the 20 nm pores are present in abundance at 0.16 cm3g-1. In contrast, the composite CAHC-0.1 predominantly contains 30-40nm pores, though the number of pores is slightly lower than in HC, with the 30nm pores accounting for approximately 0.22cm3g-1. The data indicates that both composite materials are mesopore-rich, but the composite material CAHC-0.1 exhibits a slightly lower number of holes: the number of 30nm pores is approximately 0.22 cm3g-1. The results indicate that mesoporous materials are present, but the composite CAHC-0.1 exhibits comparatively larger mesopore diameters and superior properties (Li et al., 2024).

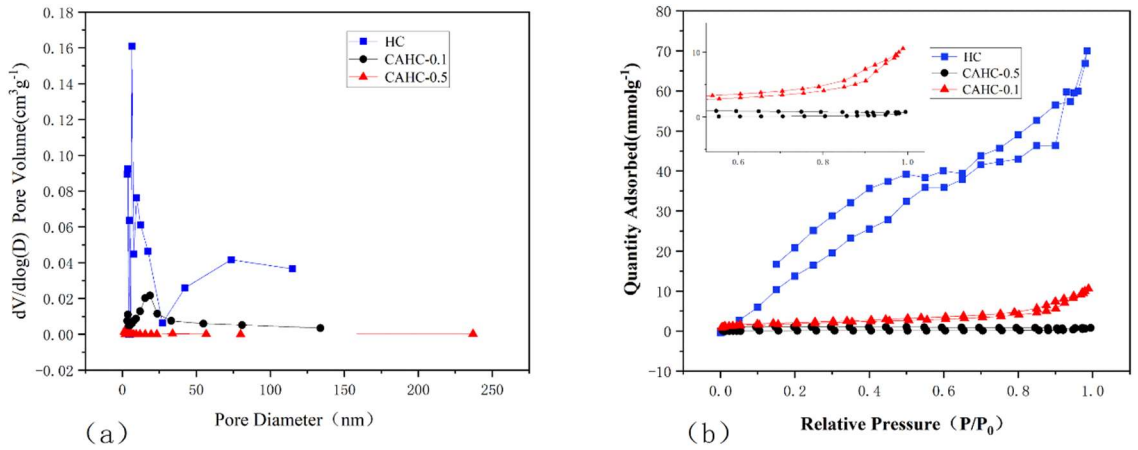

Fig. 6. The N2 desorption isotherms and pore size distribution of HC, CAHC-0.1 and CAHC-0.5

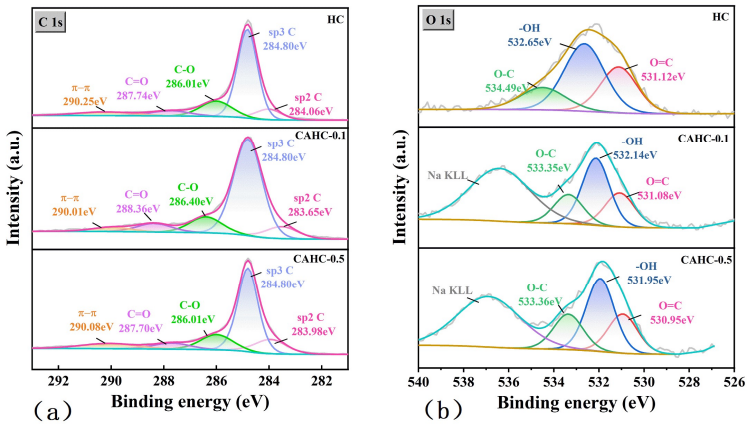

Fig. 7. (a) Infrared test image of CAHC-0.1; (b) CV curves of the CAHC-0.1; (c) Charge discharge blue cycle diagram of CAHC-0.1; (d) Blue charge discharge rate chart of CAHC-0.1

The XPS images of HC, CAHC-0.1, and CAHC-0.5 are displayed in Fig. 7(a) presents the XPS image of material C element, exhibiting a peak of sp3C at 284.80 eV and a peak of sp2C at 284.06 eV. Concurrently, a peak of C=O is observed at 288.74 eV, and a peak of C-O bond is observed at 286.01 eV. Fig. 7(b) shows the XPS image of the O element in the material, with the -OH. As can be seen in

ISSN: 2414-1895 DOI: 10.6919/ICJE.202505_11(5).0031

Fig. 7(b), the XPS image of the O element in the material shows the -OH bond peak at 532.14 eV, the O=C bond peak at 531.08 eV, the O-C bond peak at 533.35 eV, and the nearby measured Na KLL peak, indicating a small impurity in citric acid. The XPS image shows that citric acid is uniformly doped into corn starch (Luo et al., 2018).

As illustrated in Fig. 8(a), the initial charge discharge curve of the hard carbon sample at a current density of 30 mA/g demonstrates an enhancement in both the initial charge and discharge capacity of pure corn starch material compared to the hard carbon sample doped with citric acid.

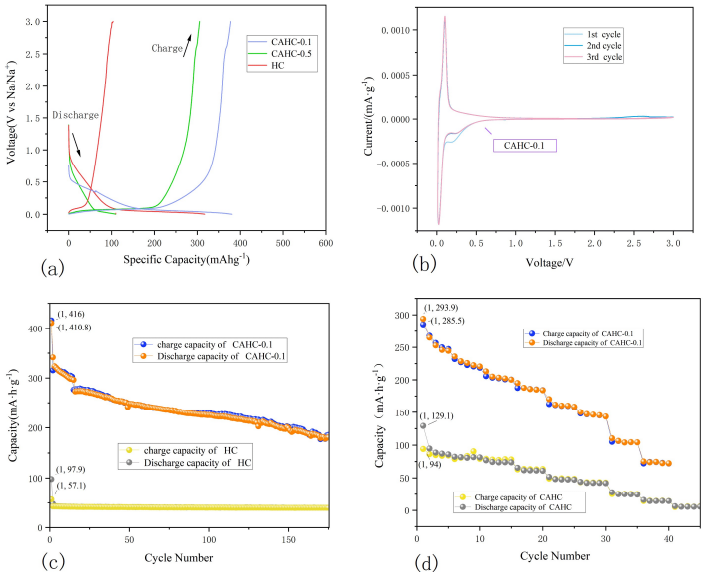

Fig.8. (a) Charge-discharge profiles of HC, CAHC-0.1, CAHC-0.5; (b) the first three CV curves of CAHC-0.1 at 0.1 mV/S; (c) Charge-discharge cycle curve of HC and CAHC-0.1; (d) Charge - discharge rate curve of HC and CAHC-0.1

The initial three-turn CV curves of the CAHC-0.1 electrode at a sweep rate of 0.1 mV/s in the button half-cell are presented in Fig. 8. The initial turn CV curve displays a discernible reduction peak, indicating that corn starch and its composites are approximately -0.00025, which is attributable to the decomposition of the electrolyte and the formation of the SEI film during the initial discharge, resulting in irreversible sodium storage capacity (Lu et al., 2017). The second and third turns of the CV curves show a pair of reversible redox peaks between -0.00025 and 0V, which corresponds to the embedding and disembedding of Na+. The CV curves of the last two turns overlap almost completely, indicating excellent reversibility in the sodium storage behavior of CAHC-0.1 (Jiang et al., 2016), which is consistent with the analytical results of the constant-current charge-discharge test (Natarajan & Aravindan, 2019).

Fig. 8(c) The graph illustrates the charge-discharge cycling performance of a button battery composed of pure cornstarch hard carbon material, evaluated at a current density of 300 mAg-1. The unique carbon structure of starch is characterized by a substantial presence of defects (Soltani et al., 2021) and interstices, which have been shown to result in significant electrolyte consumption during the charging and discharging processes (Tang et al., 2017). This phenomenon leads to the formation of numerous dead sodium sites within the cell, consequently enhancing the irreversible capacity (Liedel, 2020). These factors contribute to the initial low coulombic efficiency of hard carbon. Consequently, the investigation of corn starch as a hard carbon anode material is imperative to address this critical issue. As demonstrated in Fig. 8(c), the initial charging specific capacity of the corn starch-based hard carbon composite is a primary concern.

The capacity of CAHC-0.1 was found to be 416.0 mAhg-1, with the initial discharging specific capacity measuring 410.8 mAhg-1 and an initial efficiency of 98.75%. Notably, the capacity remains

ISSN: 2414-1895 DOI: 10.6919/ICJE.202505_11(5).0031

consistent after 100 cycles, and the charging specific capacity after 120 cycles is recorded at 222.2 mAhg-1, while the discharge specific capacity is 217 mAhg-1. In comparison with the pure corn starch material, the initial charging specific capacity is 57.1 mAhg-1, the initial discharging specific capacity is 97.9 mAhg-1, and the charging specific capacity is only 40.1 mAhg-1 after the 120th cycle. It is evident that, in comparison with the pure corn starch material, the batteries composed of corn starch-based hard carbon composites CAHC-0.1 exhibit a significant enhancement in both the initial charge/discharge specific capacity and the initial efficiency (Sekar et al., 2020).

Furthermore, these batteries demonstrate a notable capacity retention even after 100 cycles (Reis et al., 2023). This finding indicates that the incorporation of citric acid-doped corn starch-based hard carbon composites can effectively enhance the reversible capacity and cycling stability of the materials.

The Fig. 8(d) demonstrates the charging and discharging multiplicity performance of button batteries composed of a corn starch-based hard carbon composite (CAHC-0.1), fabricated at current densities ranging from 20 to 1500 mAg-1. As demonstrated in Table 2, the initial efficiency of the corn starch-based hard carbon composite CAHC-0.1 was 97.15%, and its specific charging capacity (given that the specific charging and discharging capacities are nearly equivalent, the specific charging capacity is employed as a representative example) at 20, 60, 120, 240, 600, and 1,500 mAg-1 current densities were 285.5, 232, 205.6, 162.7, 105, and 72.2 mAhg-1. However, as demonstrated in Table 2, the initial efficiency of the pure phase corn starch hard carbon material is 72.79%, and its capacity under the same multiplicity current density is 94, 78.8, 79.3, 43.5, 14.2 and 5 mAg-1. The findings of this study demonstrate the efficacy of citric acid-doped corn starch-based hard carbon composites in enhancing the capacity of the material under high current density conditions (Tian et al., 2019).

Table 2. First Coulombic Efficiency of HC, CAHC-0.1 and CAHC-0.5

	Efficiency of the first round of the cycle(%)	Efficiency of the first round of multiplication (%)
HC	58.32	72.79
CAHC-0.1	101.27	97.15

4. Conclusion

In conclusion, hard carbon composites were prepared by doping citric acid using corn starch as a precursor, followed by calcination and further processing. It is evident that the cells prepared by CAHC-0.1 exhibit a higher capacity. Consequently, the hard carbon composite material prepared with a doping amount of 2g is advantageous in enhancing the performance of sodium ion batteries. This material is regarded as one of the most promising candidates for industrialization in the sodium electricity market.

Acknowledgments

This work was generously supported by the State Key Laboratory of Precision Electronic Manufacturing Technology and Equipment, Guangdong University of Technology, China.

Author contributions

This article is the author's original idea, and the experimental implementation, data processing, and paper writing were all completed by the author herself.

Declaration of interests

No potential conflict of interest was reported by the author.

ISSN: 2414-1895 DOI: 10.6919/ICJE.202505_11(5).0031

References

[1] Arie, A. A., Tekin, B., Demir, E., & Demir-Cakan, R. (2019). Hard carbons derived from waste tea bag powder as anodes for sodium ion battery. Materials Technology, 34(9), 515-524. doi:10.1080/10667857.2019.1586087.

[2] Cao, L. Y., Hui, W. L., Xu, Z. W., Huang, J. F., Zheng, P., Li, J. Y., & Sun, Q. Q. (2017). Rape seed shuck derived-lamellar hard carbon as anodes for sodium-ion batteries. Journal of Alloys and Compounds, 695, 632-637. doi:10.1016/j.jallcom.2016.11.135.

[3] Chen, J. W., Adit, G., Li, L., Zhang, Y. X., Chua, D. H. C., & Lee, P. S. (2023). Optimization Strategies Toward Functional Sodium-Ion Batteries. Energy & Environmental Materials, 6(4). doi:10.1002/eem2.12633.

[4] Chen, S. J., Tang, K. J., Song, F., Liu, Z. C., Zhang, N., Lan, S. L., ... Wu, Z. J. (2022). Porous hard carbon spheres derived from biomass for high-performance sodium/potassium-ion batteries. Nanotechnology, 33(5). doi:10.1088/1361-6528/ac317d.

[5] Dong, S. Y., Lv, N., Wu, Y. L., Zhang, Y. Z., Zhu, G. Y., & Dong, X. C. (2022). Titanates for sodium-ion storage. Nano Today, 42. doi:10.1016/j.nantod.2021.101349.

[6] dos Reis, G. S., Molaiyan, P., Subramaniyam, C. M., García-Alvarado, F., Paolella, A., de Oliveira, H. P., & Lassi, U. (2023). Biomass-derived carbon-silicon composites (C@Si) as anodes for lithium-ion and sodium-ion batteries: A promising strategy towards long-term cycling stability: A mini review. Electrochemistry Communications, 153. doi:10.1016/j.elecom.2023.107536.

[7] El Moctar, I., Ni, Q., Bai, Y., Wu, F., & Wu, C. (2018). Hard carbon anode materials for sodium-ion batteries. Functional Materials Letters, 11(6). doi:10.1142/s1793604718300037.

[8] Fan, X. Y., Kong, X. R., Zhang, P. T., & Wang, J. L. (2024). Research progress on hard carbon materials in advanced sodium-ion batteries. Energy Storage Materials, 69. doi:10.1016/j.ensm.2024.103386.

[9] Gao, X. P., An, Y. L., Zhang, W. S., Yu, M. L., Ci, L. J., & Feng, J. K. (2018). Self-supporting soft carbon fibers as binder-free and flexible anodes for high-performance sodium-ion batteries. Materials Technology, 33(12), 810-814. doi:10.1080/10667857.2018.1509525.

[10] Guo, S., Chen, Y. M., Tong, L. P., Cao, Y., Jiao, H., Long, Z., & Qiu, X. Q. (2022). Biomass hard carbon of high initial coulombic efficiency for sodium-ion batteries: Preparation and application. Electrochimica Acta, 410. doi:10.1016/j.electacta.2022.140017.

[11] Jiang, Q., Zhang, Z. H., Yin, S. Y., Guo, Z. P., Wang, S. Q., & Feng, C. Q. (2016). Biomass carbon micro/nano-structures derived from ramie fibers and corncobs as anode materials for lithium-ion and sodium-ion batteries. Applied Surface Science, 379, 73-82. doi:10.1016/j.apsusc.2016.03.204.

[12] Kim, K., Lim, D. G., Han, C. W., Osswald, S., Ortalan, V., Youngblood, J. P., & Pol, V. G. (2017). Tailored Carbon Anodes Derived from Biomass for Sodium-Ion Storagel. Acs Sustainable Chemistry & Engineering, 5(10), 8720-8728. doi:10.1021/acssuschemeng.7b01497.

[13] Kumar, D. R., Kanagaraj, I., Dhakal, G., Prakash, A. S., & Shim, J. J. (2021). Palmyra Palm tree biomass-derived carbon low-voltage plateau region capacity on Na-ion battery and its full cell performance. Journal of Environmental Chemical Engineering, 9(4). doi:10.1016/j.jece.2021.105698.

[14] Kumaresan, T. K., Masilamani, S. A., Raman, K., Karazhanov, S. Z., & Subashchandrabose, R. (2021). High performance sodium-ion battery anode using biomass derived hard carbon with engineered defective sites. Electrochimica Acta, 368. doi:10.1016/j.electacta.2020.137574.

[15] Lakienko, G. P., Bobyleva, Z. V., Apostolova, M. O., Sultanova, Y. V., Dyakonov, A. K., Zakharkin, M. V., ... Antipov, E. V. (2022). Sosnowskyi Hogweed-Based Hard Carbons for Sodium-Ion Batteries. Batteries-Basel, 8(10). doi:10.3390/batteries8100131.

[16] Li, Q., Wu, M. Y., Wang, Y., Wang, G. X., Zhuo, L. H., & Li, Z. Q. (2021). Untra-high pseudocapacitance enhanced anode of N, P dual-doped carbon nanosheet derived from biomass toward high performance sodium ion battery. Nano Select, 2(1), 129-139. doi:10.1002/nano.202000114.

[17] Li, R. Z., Huang, J. F., Xu, Z. W., Qi, H., Cao, L. Y., Liu, Y. J., ... Li, J. Y. (2018). Controlling the Thickness of Disordered Turbostratic Nanodomains in Hard Carbon with Enhanced Sodium Storage Performance. Energy Technology, 6(6), 1080-1087. doi:10.1002/ente.201700674.

ISSN: 2414-1895 DOI: 10.6919/ICJE.202505_11(5).0031

[18] Li, W. B., Chen, M. M., & Wang, C. Y. (2011). Spherical hard carbon prepared from potato starch using as anode material for Li-ion batteries. Materials Letters, 65(23-24), 3368-3370. doi:10.1016/j.matlet.2011.07.072.

[19] Li, Y. L., Xia, D. W., Tao, L., Xu, Z. Y., Yu, D. J., Jin, Q., ... Huang, H. B. (2024). Hydrothermally Assisted Conversion of Switchgrass into Hard Carbon as Anode Materials for Sodium-Ion Batteries. Acs Applied Materials & Interfaces, 16(22), 28461-28472. doi:10.1021/acsami.4c02734.

[20] Liedel, C. (2020). Sustainable Battery Materials from Biomass. Chemsuschem, 13(9), 2110-2141. doi:10.1002/cssc.201903577.

[21] Lin, M., Deng, M. D., Zhou, C. J., Shu, Y. J., Yang, L. C., Ouyang, L. Z., ... Zhu, M. (2019). Popcorn derived carbon enhances the cyclic stability of MoS2 as an anode material for sodium-ion batteries. Electrochimica Acta, 309, 25-33. doi:10.1016/j.electacta.2019.04.070.

[22] Lu, M. J., Yu, W. H., Shi, J., Liu, W., Chen, S. G., Wang, X., & Wang, H. L. (2017). Self-doped carbon architectures with heteroatoms containing nitrogen, oxygen and sulfur as high-performance anodes for lithium-and sodium-ion batteries. Electrochimica Acta, 251, 396-406. doi:10.1016/j.electacta.2017.08.131.

[23] Luo, D. H., Han, P., Shi, L. D., Huang, J. T., Yu, J. L., Lin, Y. M., ... Xu, J. (2018). Biomass-derived nitrogen/oxygen co-doped hierarchical porous carbon with a large specific surface area for ultrafast and long-life sodium-ion batteries. Applied Surface Science, 462, 713-719. doi:10.1016/j.apsusc.2018.08.106.

[24] Natarajan, S., Lee, Y. S., & Aravindan, V. (2019). Biomass-Derived Carbon Materials as Prospective Electrodes for High-Energy Lithium- and Sodium-Ion Capacitors. Chemistry-an Asian Journal, 14(7), 936-951. doi:10.1002/asia.201900030.

[25] Nayak, P. K., Yang, L. T., Brehm, W., & Adelhelm, P. (2018). From Lithium-Ion to Sodium-Ion Batteries: Advantages, Challenges, and Surprises. Angewandte Chemie-International Edition, 57(1), 102-120. doi:10.1002/anie.201703772.

[26] Pang, Z. W., Wang, L. T., Wan, S. T., Liu, M. M., Niu, X. H., Wang, K. J., & Li, H. X. (2024). Wedelia chinensis-derived biomass porous carbon as anode material for high performance sodium/potassium-ion batteries. Ionics. doi:10.1007/s11581-024-05604-3.

[27] Sekar, S., Ahmed, A. A., Kim, D. Y., & Lee, S. (2020). One-Pot Synthesized Biomass C-Si Nanocomposites as an Anodic Material for High-Performance Sodium-Ion Battery. Nanomaterials, 10(9). doi:10.3390/nano10091728.

[28] Shen, G. Y., Li, B. C., Xu, Y. Y., Chen, X. Z., Katiyar, S., Zhu, L. M., ... Cao, X. Y. (2024). Waste biomass garlic stem-derived porous carbon materials as high-capacity and long-cycling anode for lithium/sodium-ion batteries. Journal of Colloid and Interface Science, 653, 1588-1599. doi:10.1016/j.jcis.2023.09.150.

[29] Soltani, N., Bahrami, A., Giebeler, L., Gemming, T., & Mikhailova, D. (2021). Progress and challenges in using sustainable carbon anodes in rechargeable metal-ion batteries. Progress in Energy and Combustion Science, 87. doi:10.1016/j.pecs.2021.100929.

[30] Tan, S. C., Yang, H., Zhang, Z., Xu, X. Y., Xu, Y. Y., Zhou, J., ... Zhang, Y. (2023). The Progress of Hard Carbon as an Anode Material in Sodium-Ion Batteries. Molecules, 28(7). doi:10.3390/molecules28073134.

[31] Tang, W. J., Zhang, Y. F., Zhong, Y., Shen, T., Wang, X. L., Xia, X. H., & Tu, J. P. (2017). Natural biomass-derived carbons for electrochemical energy storage. Materials Research Bulletin, 88, 234-241. doi:10.1016/j.materresbull.2016.12.025.

[32] Tian, W. F., Wang, L., Huo, K. F., & He, X. M. (2019). Red phosphorus filled biomass carbon as high-capacity and long-life anode for sodium-ion batteries. Journal of Power Sources, 430, 60-66. doi:10.1016/j.jpowsour.2019.04.086.

[33] Wang, C. W., Huang, J. F., Li, Q. Y., Cao, L. Y., Li, J. Y., & Kajiyoshi, K. (2020). Catalyzing carbon surface by Ni to improve initial coulombic efficiency of sodium-ion batteries. Journal of Energy Storage, 32. doi:10.1016/j.est.2020.101868.

[34] Wang, D. X., Bie, X. F., Fu, Q., Dixon, D., Bramnik, N., Hu, Y. S., ... Du, F. (2017). Sodium vanadium titanium phosphate electrode for symmetric sodium-ion batteries with high power and long lifespan. Nature Communications, 8. doi:10.1038/ncomms15888.

ISSN: 2414-1895 DOI: 10.6919/ICJE.202505_11(5).0031

[35] Wang, J., Li, Y. S., Liu, P., Wang, F., Yao, Q. R., Zou, Y. J., ... Deng, J. Q. (2021). Green large-scale production of N/O-dual doping hard carbon derived from bagasse as high-performance anodes for sodium-ion batteries. Journal of Central South University, 28(2), 361-369. doi:10.1007/s11771-021-4608-y.

[36] Wang, J. R., Xi, L., Peng, C. X., Song, X., Wan, X. H., Sun, L. Y., ... Liu, J. (2024). Recent Progress in Hard Carbon Anodes for Sodium-Ion Batteries. Advanced Engineering Materials, 26(8). doi:10.1002/adem.202302063.

[37] Wang, P. T., Wang, H. A., Liang, C., & Yu, K. F. (2023). Two-dimensional porous flake biomass carbon with large layer spacing as an anode material for sodium ion batteries. Diamond and Related Materials, 131. doi:10.1016/j.diamond.2022.109601.

[38] Yan, J. K., Li, Q. Y., Hao, Y., Dai, C., & Chen, Y. (2020). MoS2/SnS2 nanocomposite as stable sodium-ion battery anode. Functional Materials Letters, 13(1). doi:10.1142/s1793604719500954.

[39] Yin, T. Q., Zhang, Z. L., Xu, L. Z., Li, C., & Han, D. D. (2024). Preparation of green high-performance biomass-derived hard carbon materials from bamboo powder waste. Chemistryopen, 13(5). doi:10.1002/open.202300178.

[40] Yu, D. Y. W., Prikhodchenko, P. V., Mason, C. W., Batabyal, S. K., Gun, J., Sladkevich, S., ... Lev, O. (2013). High-capacity antimony sulphide nanoparticle-decorated graphene composite as anode for sodium-ion batteries. Nature Communications, 4. doi:10.1038/ncomms3922.

[41] Zhang, F., Yao, Y. G., Wan, J. Y., Henderson, D., Zhang, X. G., & Hu, L. B. (2017). High Temperature Carbonized Grass as a High Performance Sodium Ion Battery Anode. Acs Applied Materials & Interfaces, 9(1), 391-397. doi:10.1021/acsami.6b12542.

[42] Zhang, J. H., Zhang, D. L., Li, K., Tian, Y. X., Wang, Y., & Sun, T. (2021). N, O and S co-doped hierarchical porous carbon derived from a series of samara for lithium and sodium storage: Insights into surface capacitance and inner diffusion. Journal of Colloid and Interface Science, 598, 250-259. doi:10.1016/j.jcis.2021.04.047.

[43] Zhu, Y. D., Huang, Y., Chen, C., Wang, M. Y., & Liu, P. B. (2019). Phosphorus-doped porous biomass carbon with ultra-stable performance in sodium storage and lithium storage. Electrochimica Acta, 321. doi:10.1016/j.electacta.2019.134698.